Geophysical Journal International

Analysis of lithospheric magnetisation in vector spherical harmonics

Journal:	*Geophysical Journal International*
Manuscript ID:	Draft
Manuscript Type:	Research Paper
Date Submitted by the Author:	n/a
Complete List of Authors:	Gubbins, David; University of Leeds, School of Earth & Environment Ivers, David; University of Sydney, Maths Masterton, Sheona; University of Leeds, School of Earth and Environment Winch, D; University of Sydney, Maths
Keywords:	Magnetic anomalies: modelling and interpretation < GEOMAGNETISM and ELECTROMAGNETISM, Satellite magnetics < GEOMAGNETISM and ELECTROMAGNETISM, Geopotential theory < GEODESY and GRAVITY

submitted to *Geophys. J. Int.*

Analysis of Lithospheric Magnetisation in Vector Spherical Harmonics.

D. Gubbins[1], D. Ivers[2], S. M. Masterton[1] & D. E. Winch[2]

[1] *School of Earth and Environment, University of Leeds, Leeds LS2 9JT, UK*

[2] *School of Mathematics and Statistics, University of Sydney, NSW 2006, Australia*

Key words: Magnetic satellites, crustal magnetisation, vector spherical harmonics, inversion

SUMMARY

The lithospheric contribution to the geomagnetic field arises from magnetised rocks in a thin shell at the Earth's surface. The lithospheric field can be calculated as an integral of the distribution of magnetisation using standard results from potential theory. Inversion of the magnetic field for the magnetisation suffers from a fundamental non-uniqueness: many important distributions of magnetisation yield no potential magnetic field outside the shell. We represent the vertically integrated magnetisation (VIM) in terms of vector spherical harmonics that are new to geomagnetism. These vector functions are orthogonal and complete over the sphere: one subset ($\mathcal{I}$) represents the part of the magnetisation that produces a potential field outside the shell, the observed field; another subset ($\mathcal{E}$) produces a potential field exclusively inside the shell; and a third, toroidal, subset ($\mathcal{T}$) produces a non-potential field associated with a radial electric current. $\mathcal{E}$ and $\mathcal{T}$ together span the null space of the inverse problem for magnetisation with perfect, complete data. We apply the theory to a recent global model of vertically integrated magnetisation, give an efficient algorithm for finding the lithospheric field, and show that our model of

magnetisation is dominated by $\mathcal{E}$, the part producing a potential field inside the shell. This is largely because, to a first approximation, the model was formed by magnetising a shell with a substantial uniform component by an internal potential field. The null space for inversion of magnetic field for VIM is therefore huge.

1 BACKGROUND

The geomagnetic field comprises 3 main parts, the main field that originates in the core dynamo, the lithospheric field that originates in magnetised rocks in a thin surface shell that is cooler than the Curie temperature, and the external field. To some extent these can be separated using the spatial and temporal spectra: the main field is large scale and varies on a long time scale, the lithospheric field is small scale and permanent, and the external field varies rapidly in time. Unfortunately there are no holes in the spectra, the different components overlap, so complete separation is impossible. This has led to some recent attempts to determine the lithospheric field from first principles by determining the magnetisation from the geology and known magnetic properties of rocks (Meyer et al., 1983; Hemant & Maus, 2005). The magnetisations can be fine-tuned to improve the match to the observed field, but formal inversion of the magnetic field for a model of the magnetisation is frustrated by a fundamental non-uniqueness. It is well known that many important distributions of magnetisation produce no magnetic field external to the magnetised shell; these distributions cannot be inferred from magnetic data.

In this paper we address the calculation of magnetic field from a distribution of magnetisation and its inverse in spherical geometry. The results are relevant to the interpretation of global data, notably the new influx of satellite-derived models of the lithospheric field. In Section 2 we give the integrals for determining the potential fields caused by a magnetised shell. In Section 3 we present a set of vector spherical harmonics that may be used to decompose any spherical distribution of magnetisation into parts that produce observable potential magnetic fields and parts that do not; the set is complete on the sphere and therefore provides a complete description of the non-uniqueness involved in any inversion of magnetic field data for VIM in spherical geometry. In Section 4 we apply the decomposition to a model of magnetisation that does a reasonable job of accounting for the satellite-derived lithospheric field, then present that part of the magnetisation responsible for the field alongside two further parts that produce no external field. In Section 5 we discuss the implications for interpretation and inversion of magnetic field for models of lithospheric magnetisation.

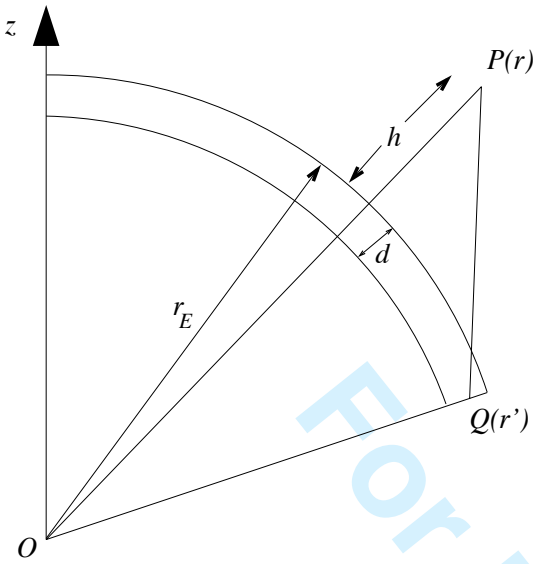

Figure 1. The magnetic potential is evaluated at field point $P(\boldsymbol{r})$ at a height h above the surface $r' = r_{\rm E}$ by summing contributions from a magnetised layer inside the sphere above a depth d. Source point $Q(\boldsymbol{r}')$ has magnetisation $\boldsymbol{M}(\boldsymbol{r}')$; distance PQ is $|\boldsymbol{r} - \boldsymbol{r}'|$.

2 THE MAGNETIC POTENTIAL DUE TO A SPHERICAL SHELL OF MAGNETISED MATERIAL.

We first address the problem of determining the magnetic field associated with a spherical shell of magnetised material with magnetisation $\boldsymbol{M}(r', \theta', \phi')$, where (r', θ', ϕ') are spherical polar coordinates. The magnetic potential at point $\boldsymbol{r}$ caused by a distribution of magnetisation $\boldsymbol{M}$ is

$$V(\boldsymbol{r}) = \frac{\mu_0}{4\pi} \int \boldsymbol{M}(\boldsymbol{r}') \cdot \nabla' \left(\frac{1}{|\boldsymbol{r} - \boldsymbol{r}'|} \right) dv', \tag{1}$$

where the integral is performed over the magnetised region [see equation (5.2) of Blakely (1995)]. We wish to find the potential at some field point $\boldsymbol{r}$ external to a magnetised shell immediately below the Earth's surface at $r = r_{\rm E}$; Figure 1 gives the geometry. Equation (1) also applies for the potential field inside the shell.

The geomagnetic potential is written as

$$\begin{aligned} V(\boldsymbol{r}) &= r_{\rm E} \sum_{l,m} \left(\frac{r_{\rm E}}{r} \right)^{l+1} P_l^m(\cos\theta)(g_l^m \cos m\phi + h_l^m \sin m\phi) \\ &= r_{\rm E} \sum_{l,m} \left(\frac{r_{\rm E}}{r} \right)^{l+1} (g_l^m Y_l^{mc} + h_l^m Y_l^{ms}), \end{aligned} \tag{2}$$

where P_l^m is a Schmidt-normalised associated Legendre function [see, e.g., Jacobs (1994)] and $Y_l^{m[c,s]}$ are real spherical harmonics, described in more detail in Appendix A. Orthogonality of the spherical harmonics may be used to write the geomagnetic coefficients as

$$[g_l^m, h_l^m] = \frac{1}{r_\mathrm{E}} \left(\frac{r}{r_\mathrm{E}}\right)^{l+1} \frac{2l+1}{4\pi} \oint V(\boldsymbol{r}) Y_l^{m[c,s]} d\Omega. \tag{3}$$

Substituting equation (1) for the potential $V(\boldsymbol{r})$ into (3) gives a double integral for the geomagnetic coefficients in terms of the magnetisation:

$$[g_l^m, h_l^m] = \frac{\mu_0}{4\pi} \frac{(2l+1)}{4\pi} \frac{1}{r_\mathrm{E}} \left(\frac{r}{r_\mathrm{E}}\right)^{l+1} \oint_\Omega \int_{r_\mathrm{E}-d}^{r_\mathrm{E}} \oint_{\Omega'} \boldsymbol{M}(r',\theta',\phi') \cdot \nabla' \left(\frac{Y_l^{m[c,s]}(\theta,\phi)}{|\boldsymbol{r}-\boldsymbol{r}'|} \right) d\Omega' r'^2 dr' d\Omega \tag{4}$$

Changing the order of the Ω and Ω' integrations gives

$$[g_l^m, h_l^m] = \frac{\mu_0}{4\pi} \frac{(2l+1)}{4\pi} \frac{1}{r_\mathrm{E}} \left(\frac{r}{r_\mathrm{E}}\right)^{l+1} \oint_{\Omega'} \int_{r_\mathrm{E}-d}^{r_\mathrm{E}} \boldsymbol{M}(r',\theta',\phi') \cdot \nabla' \left[\oint \frac{Y_l^{m[c,s]}(\theta,\phi)}{|\boldsymbol{r}-\boldsymbol{r}'|} d\Omega \right] r'^2 dr' d\Omega' \tag{5}$$

The inner integral is now in standard form and may be obtained from the formula for the generating function for spherical harmonics [see Appendix B]. Two formulae are possible, corresponding to the cases $r > r'$ and $r < r'$. For the observable geomagnetic field we need the former, given by equation (B.8):

$$\oint \frac{Y_l^{m[c,s]}(\theta,\phi)}{|\boldsymbol{r}-\boldsymbol{r}'|} d\Omega = \frac{4\pi}{2l+1} \frac{1}{r} \left(\frac{r'}{r}\right)^l Y_l^{m[c,s]}(\theta',\phi'). \tag{6}$$

Substituting into (5) and cancelling factors of r, which are not integrated over or differentiated, gives

$$[g_l^m, h_l^m] = \frac{\mu_0}{4\pi} \frac{1}{r_\mathrm{E}^l} \oint_{\Omega'} \int_{r_\mathrm{E}-d}^{r_\mathrm{E}} \boldsymbol{M}(r',\theta',\phi') \cdot \nabla' \left[r'^l Y_l^{m[c,s]}(\theta',\phi') \right] r'^2 dr' d\Omega'. \tag{7}$$

2.1 Radial Integration

Define the radial *l-moments* of magnetisation as

$$\bar{\boldsymbol{M}}_l(\theta',\phi') = \frac{1}{r_\mathrm{E}^l} \int_{r_\mathrm{E}-d}^{r_\mathrm{E}} r'^l \boldsymbol{M}(r',\theta',\phi') dr'. \tag{8}$$

Write the integral (7) as

$$[g_l^m, h_l^m] = \frac{\mu_0}{4\pi} \frac{1}{r_\mathrm{E}^{l+2}} \oint_{\Omega'} \int_{r_\mathrm{E}-d}^{r_\mathrm{E}} r'^{l+1} \boldsymbol{M}(r',\theta',\phi') \cdot \left\{ \frac{1}{r'^{l-1}} \nabla' \left[r'^l Y_l^{m[c,s]}(\theta',\phi') \right] \right\} dr' d\Omega'. \tag{9}$$

and note that the term in curly brackets is independent of r' when the gradient is taken. The radial integration then yields the moment $\bar{\boldsymbol{M}}_{l+1}$:

$$[g_l^m, h_l^m] = \frac{\mu_0}{4\pi} \frac{1}{r_\mathrm{E}} \oint_{\Omega'} \bar{\boldsymbol{M}}_{l+1}(\theta',\phi') \cdot \frac{1}{r'^{l-1}} \nabla' \left[r'^l Y_l^{m[c,s]}(\theta',\phi') \right] d\Omega', \tag{10}$$

If the magnetised layer is sufficiently thin and l is small the radial moments may be replaced by a single *vertically integrated magnetisation* (VIM), $\bar{\boldsymbol{M}}_{l+1} = \bar{\boldsymbol{M}}_0$, or simply $\bar{\boldsymbol{M}}$. This always underweights the deep magnetisation since $\bar{\boldsymbol{M}}_{l+1} < \bar{\boldsymbol{M}}_0$, and the error increases with spherical harmonic degree. For a thin layer, $d \ll r_\mathrm{E}$, we have, with $x = r_\mathrm{E} - r'$:

$$|\bar{\boldsymbol{M}}_0 - \bar{\boldsymbol{M}}_l| = \int_{r_\mathrm{E}-d}^{r_\mathrm{E}} |\boldsymbol{M}| \left[1 - \left(\frac{r'}{r_\mathrm{E}}\right)^l \right] dr'$$

$$\approx \int_0^d |\boldsymbol{M}| \left[l\frac{x}{r_{\rm E}} - \frac{l\,(l-1)}{2}\left(\frac{x}{r_{\rm E}}\right)^2 + \ldots \right] dx. \tag{11}$$

The small parameter is therefore $ld/r_{\rm E}$, and to leading order the relative error is $O(ld/r_{\rm E})$. Taking $d = 50$ km as the depth of the magnetised layer and $r_{\rm E} = 6371$ km shows that the error becomes large well before $l = 100$. This could be an overestimate for a number of reasons. First, d is rarely as thick as 50 km. Secondly, the factor r'^l is concentrated more towards the top of the integration range, increasingly so as l increases, reflecting the stronger influence of near-surface magnetisation on the shorter wavelengths, and the magnetisation may be concentrated in shallower depths where the effect of the factor r'^l is weakest. For the rest of this paper we use the VIM, $\bar{\boldsymbol{M}}$, as an approximation for the correct moments.

2.2 The field internal to the shell

For completeness consider the magnetic potential inside the magnetised shell, the one finite at the origin. This has the form

$$V(\boldsymbol{r}) = r_{\rm E}\sum_{l,m}\left(\frac{r}{r_{\rm E}}\right)^l P_l^m(\cos\theta)(r_l^m\cos m\phi + s_l^m \sin m\phi), \tag{12}$$

where the $\{r_l^m, s_l^m\}$ are real coefficients analogous to the geomagnetic coefficients $\{g_l^m, h_l^m\}$. Proceeding as before, equating the magnetic potential to the integral in (1) and using orthogonality of the spherical harmonics, gives

$$[r_l^m, s_l^m] = \frac{\mu_0}{4\pi}\frac{2l+1}{4\pi}\frac{1}{r_{\rm E}}\left(\frac{r_{\rm E}}{r}\right)^l \oint_{\Omega'}\int_{r_{\rm E}-d}^{r_{\rm E}} \boldsymbol{M}\cdot\nabla'\left(\oint_\Omega \frac{Y_l^{m[c,s]}}{|\boldsymbol{r}-\boldsymbol{r}'|}d\Omega\right) r'^2 dr' d\Omega' \tag{13}$$

We now use the form of the internal integral over Ω' valid for $r < r'$, (B.9), to give

$$[r_l^m, s_l^m] = \frac{\mu_0}{4\pi}\frac{1}{r_{\rm E}}\left(\frac{r_{\rm E}}{r}\right)^l \oint_{\Omega'}\int_{r_{\rm E}-d}^{r_{\rm E}} \boldsymbol{M}\cdot\nabla'\left(\frac{r^l}{r'^{l+1}}Y_l^{m[c,s]}\right) r'^2 dr' d\Omega'. \tag{14}$$

or in terms of the l-moments

$$[r_l^m, s_l^m] = \frac{\mu_0}{4\pi r_{\rm E}}\oint_{\Omega'} \bar{\boldsymbol{M}}_{-l}\cdot\left\{r'^{l+2}\nabla'\left(\frac{1}{r'^{l+1}}Y_l^{m[c,s]}\right)\right\} d\Omega'. \tag{15}$$

Once again $\bar{\boldsymbol{M}}_{-l}$ may be replaced by $\bar{\boldsymbol{M}}$ for a thin layer provided l is not too high.

3 VECTOR SPHERICAL HARMONICS

3.1 Definition and properties

Any vector function defined on the surface of a sphere can be expanded as a sum over 3 types of orthogonal vector spherical harmonic

$$\boldsymbol{Y}_{l,l+1}^m = \frac{r^{l+2}}{\sqrt{(l+1)\,(2l+1)}}\nabla\left[\frac{1}{r^{l+1}}Y_l^m(\theta,\phi)\right] \tag{16}$$

$$\boldsymbol{Y}^m_{l,l} = -\frac{i}{\sqrt{l\,(l+1)}}\boldsymbol{r}\times\nabla Y^m_l(\theta,\phi) \tag{17}$$

$$\boldsymbol{Y}^m_{l,l-1} = \frac{1}{r^{l-1}\sqrt{l\,(2l+1)}}\nabla\left[r^l Y^m_l(\theta,\phi)\right] \tag{18}$$

Y^m_l denotes the complex mean-normalised spherical harmonics (Edmonds, 1974). See Appendix B for their relation to real Schmidt-normalised harmonics.

Their components in spherical polar coordinates are

$$(\boldsymbol{Y}^m_{l,l+1})_r = -\sqrt{\frac{l+1}{2l+1}}Y^m_l \tag{19}$$

$$(\boldsymbol{Y}^m_{l,l+1})_\theta = \frac{1}{\sqrt{(l+1)\,(2l+1)}}\frac{\partial Y^m_l}{\partial\theta} \tag{20}$$

$$(\boldsymbol{Y}^m_{l,l+1})_\phi = \frac{1}{\sqrt{(l+1)\,(2l+1)}}\frac{1}{\sin\theta}\frac{\partial Y^m_l}{\partial\phi} \tag{21}$$

$$(\boldsymbol{Y}^m_{l,l-1})_r = \sqrt{\frac{l}{2l+1}}Y^m_l \tag{22}$$

$$(\boldsymbol{Y}^m_{l,l-1})_\theta = \frac{1}{\sqrt{l\,(2l+1)}}\frac{\partial Y^m_l}{\partial\theta} \tag{23}$$

$$(\boldsymbol{Y}^m_{l,l-1})_\phi = \frac{1}{\sqrt{l\,(2l+1)}}\frac{1}{\sin\theta}\frac{\partial Y^m_l}{\partial\phi} \tag{24}$$

$$(\boldsymbol{Y}^m_{l,l})_r = 0 \tag{25}$$

$$(\boldsymbol{Y}^m_{l,l})_\theta = \frac{i}{\sqrt{l\,(l+1)}}\frac{1}{\sin\theta}\frac{\partial Y^m_l}{\partial\phi} \tag{26}$$

$$(\boldsymbol{Y}^m_{l,l})_\phi = \frac{-i}{\sqrt{l\,(l+1)}}\frac{\partial Y^m_l}{\partial\theta} \tag{27}$$

They are simply related to the vector harmonics defined by Morse & Feschbach (1953), page 1896, and, like them, form a complete, orthogonal, mean-normalised set under integration over the sphere.

We expand the VIM in these vector spherical harmonics:

$$\bar{\boldsymbol{M}}(r,\theta,\phi) = \sum_{l,m} E^m_l\boldsymbol{Y}^m_{l,l+1}(\theta,\phi) + I^m_l\boldsymbol{Y}^m_{l,l-1}(\theta,\phi) + T^m_l\boldsymbol{Y}^m_{l,l}(\theta,\phi). \tag{28}$$

The coefficients are integrals of the magnetisation; orthogonality gives

$$E^m_l = \frac{1}{4\pi}\oint\bar{\boldsymbol{M}}\cdot(\boldsymbol{Y}^m_{l,l+1})^*d\Omega \tag{29}$$

$$I^m_l = \frac{1}{4\pi}\oint\bar{\boldsymbol{M}}\cdot(\boldsymbol{Y}^m_{l,l-1})^*d\Omega \tag{30}$$

$$T^m_l = \frac{1}{4\pi}\oint\bar{\boldsymbol{M}}\cdot(\boldsymbol{Y}^m_{l,l})^*d\Omega, \tag{31}$$

where $*$ denotes the complex conjugate.

3.2 Relationship between the geomagnetic coefficients and the coefficients of the vector spherical harmonic expansion of the magnetisation

Comparing (30) and (22)–(24) with (7) shows the geomagnetic coefficients are related only to the $\{I_l^m\}$:

$$g_l^m = -\frac{\mu_0}{r_\mathrm{E}}\sqrt{l\epsilon_m}\,\mathrm{Re}(I_l^m) \tag{32}$$

$$h_l^m = \frac{\mu_0}{r_\mathrm{E}}\sqrt{l\epsilon_m}\,\mathrm{Im}(I_l^m) \tag{33}$$

where

$$\epsilon_m = 2 - \delta_{m0}. \tag{34}$$

Similarly, comparing the expression for the coefficients of the internal field (14) with (29) shows them to be related only to the coefficients $\{E_l^m\}$:

$$r_l^m = -\frac{\mu_0}{r_\mathrm{E}}\sqrt{(l+1)\,\epsilon_m}\,\mathrm{Re}(E_l^m) \tag{35}$$

$$s_l^m = \frac{\mu_0}{r_\mathrm{E}}\sqrt{(l+1)\,\epsilon_m}\,\mathrm{Im}(E_l^m). \tag{36}$$

The coefficients $\{T_l^m\}$, the toroidal part of $\widetilde{\boldsymbol{M}}$, produce a magnetic field associated with a radial electric current and are therefore zero in the electrically insulating regions outside the magnetised layer.

3.3 The null space for inversion of geomagnetic coefficients for lithospheric magnetisation

Given a model of the VIM that has already been decomposed into vector spherical harmonic coefficients, the magnetic field external to the shell may be computed trivially from the $\{I_l^m\}$ using (32) and (33). If, on the other hand, we wish to invert the magnetic field for the VIM, the standard inverse problem of geomagnetism, then this formalism shows clearly the ambiguity involved. The null space for the inverse problem is spanned by the vector harmonics $\boldsymbol{Y}_{l,l+1}^m$ and $\boldsymbol{Y}_{l,l}^m$. If we wish to invert for the magnetisation as a function of depth, a further ambiguity appears because we can only obtain one moment for each spherical harmonic degree. All moments would be needed to obtain the full depth profile of the magnetisation.

Any potential magnetic field of internal origin can be expanded in the vector harmonics $\{\boldsymbol{Y}_{l,l+1}^m\}$. This is easily seen by comparing the component form of the harmonics $\{\boldsymbol{Y}_{l,l+1}^m\}$ in (16) with the gradient of the potential for the geomagnetic field in (2). Any laterally uniform, isotropic shell magnetised by such a field will also have an expansion that only contains the $\{\boldsymbol{Y}_{l,l+1}^m\}$, whether the magnetisation is induced or remanent and regardless of its radial

dependence. The $\{I_l^m\}$ coefficients of the magnetic field are all zero for such a magnetisation, and therefore by (32) and (33) the field external to the shell is zero. This has been called Runcorn's theorem (Runcorn, 1975; Jackson, 2008) because Runcorn frequently invoked the result to explain the magnetisation of the Moon. The vector spherical harmonic formulation provides a simple and straightforward proof of the theorem.

If the magnetising layer is non-uniform no such result applies; in general there will be contributions to both I_l^m and T_l^m from a non-uniform induced or remanent layer. Rotation of remanently magnetised crust will also, in general, produce I_l^m and T_l^m components. The $\{E_l^m\}$ components are likely to dominate, however, because to a first approximation the crustal field is expected to be that of a thin uniform layer magnetised from within. This presents a huge problem for the inversion of measured magnetic fields for crustal magnetisation because most of the magnetisation produces no observable magnetic field.

4 DECOMPOSITION OF THE VIM

4.1 The magnetisation model

We now apply the formalism to a model of VIM. It comprises two parts: (a) induced magnetisation for the oceans and continents derived by Hemant & Maus (2005) and (b) remanent magnetisation for the oceans described by Masterton (2010). The induced magnetisation is based on an assignment of standard susceptibilities to major geological units with vertical integration over the seismic crustal thickness on continents and over a uniform 3-layer crust for the oceans. The degree-13 IGRF-11 was taken as the inducing field. The remanence magnetisation was derived by magnetising oceanic lithosphere at the ridge axis, applying the reversal time scale of Cande & Kent (1995), then using plate reconstruction models to rotate constant age polygons into their present position, allowing for some reduction in thermal remanence and acquisition of chemical remanence (Raymond & Labrecque, 1987). Full details of the magnetisation model and comparisons of its external potential field with satellite models is given in a companion paper (Masterson et al., 2011). The resulting VIM is shown in Figure 2.

4.2 Expansion of the magnetisation model in vector spherical harmonics

The magnetisation model was interpolated onto a $0.25 \times 0.25^\circ$ grid in order to perform the integrations in (29)–(31). The integration in ϕ and sums over m were performed by fast Fourier transform; integration over θ was performed by trapezium rule integration. The transformation

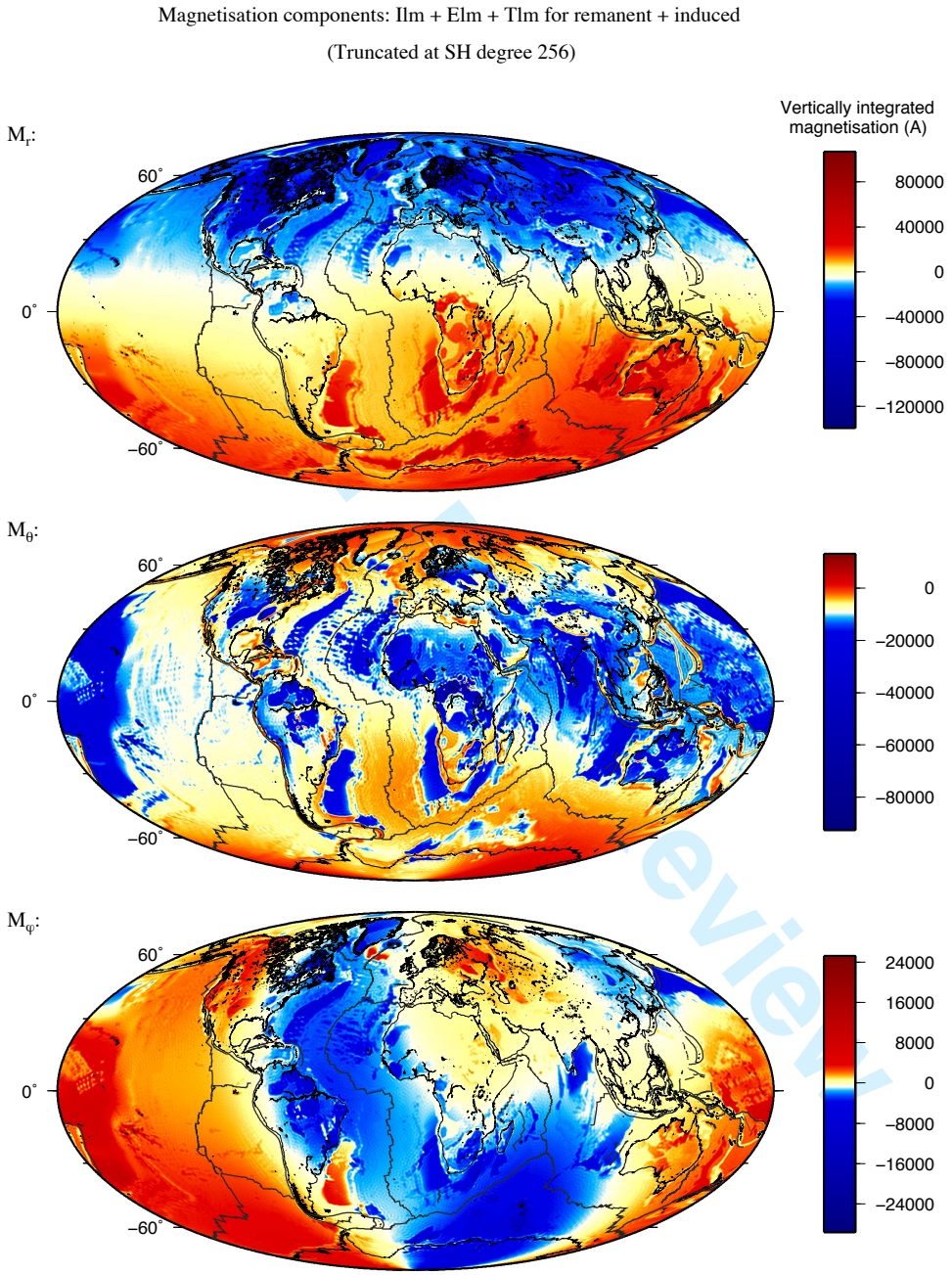

Figure 2. The vertically integrated magnetisation model used in this paper. For details on its derivation see Hemant & Maus (2005) and Masterson et al. (2011).

was immediately inverted to recover the magnetisation in space. This inverted magnetisation is not exactly equal to the original model because the spherical harmonic series was truncated at a lower level than that required for exact representation. Experiment showed that truncation at degree 256 gave satisfactory agreement with the original model.

Having the full set of vector spherical harmonic coefficients, it is a simple matter to reconstitute the 3 contributions $(\mathcal{I}, \mathcal{E}, \mathcal{T})$ to the full vector magnetisation by zeroing out unwanted coefficients before inverting the transform. The results are shown in Figures 3–6. The $\mathcal{I}$ VIM in Figure 3 is that part of the full magnetisation that produces a magnetic field external to the magnetised shell. In an inversion of observed magnetic field we can only estimate this part of the full magnetisation: it represents the minimum-norm solution of an inversion of perfect, complete data. The $\mathcal{E}+\mathcal{T}$ VIM in Figure 6 is that part of the full magnetisation that produces no magnetic field external to the shell. It could not be determined from an inversion of observed magnetic field and therefore represents an annihilator for the inverse problem. The individual subsets $\mathcal{E}$ and $\mathcal{T}$ are also annihilators, as is any linear combination of the two. Furthermore, these are the only annihilators contained in this magnetisation distribution.

5 DISCUSSION

5.1 The null space: implications for inversion of satellite data for magnetisation

The primary purpose of this paper has been to set out the formalism required to decompose crustal magnetisation into those parts that produce the observed magnetic field and those that do not. The vector spherical harmonic decomposition shows clearly that two distinct components of the magnetisation produce no external potential magnetic field, and that these are the only two such components. All of the observed magnetic field is produced by the third component of magnetisation, $\mathcal{I}$.

Comparing the scales on the figures for $\mathcal{I}$, $\mathcal{E}$ and $\mathcal{T}$ in Figures 3–6 shows $\mathcal{E}$ to be the largest. Integrating the square of each contribution to give a "surface energy" shows the 3 contributions to be $\mathcal{E}$:$\mathcal{I}$:$\mathcal{T}$ =88% :8% :4% . Only 8% of the crustal magnetisation is responsible for the observed crustal field! Furthermore, $\mathcal{E}$ in Figure 5 has a distinct axial dipole character, reflecting the dominant contribution from a uniform layer magnetised by an internal dipole: term E_1^0 dominates all other coefficients by nearly a factor of 10. The toroidal component is smallest; it arises partly from rotation of remanently magnetised crust but only when that rotation changes the direction of magnetisation.

Any inversion of satellite magnetic field for magnetisation will suffer from serious non-

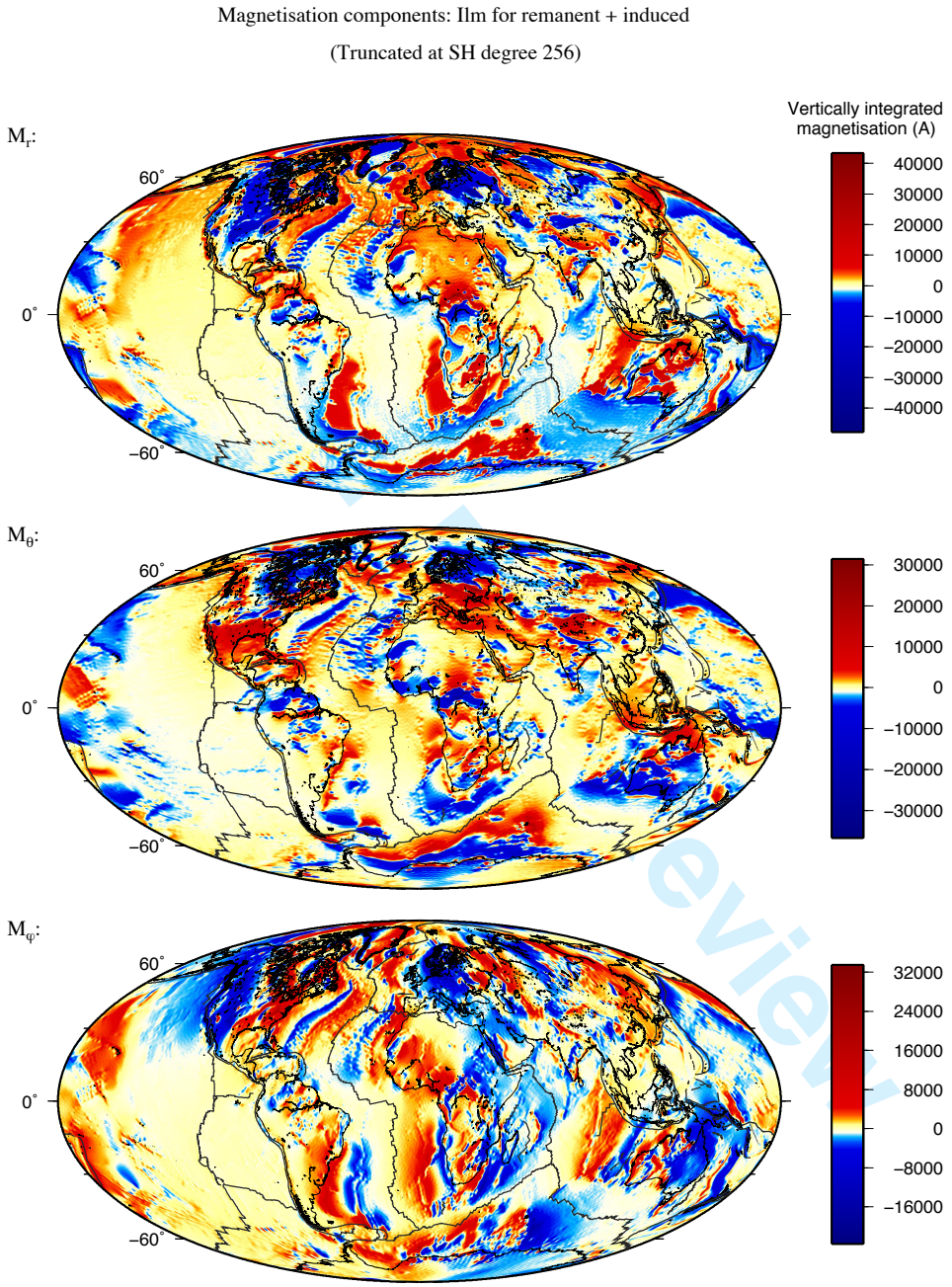

Figure 3. The $\mathcal{I}$ component of VIM obtained by summing only the I_l^m terms in (28). This is the only component of VIM that produces a potential magnetic field outside the shell.

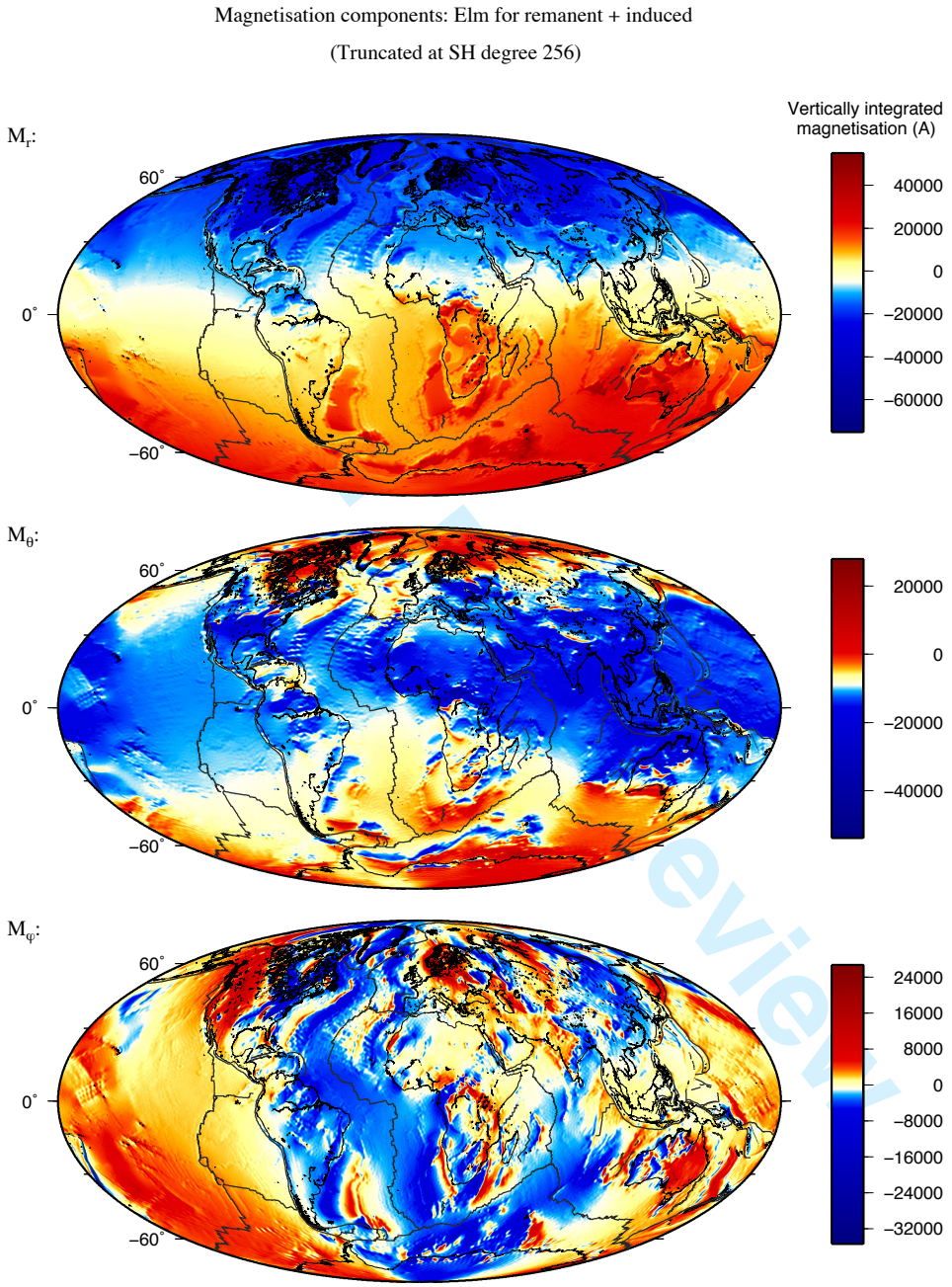

Figure 4. As Figure 3 for the $\mathcal{E}$ component of VIM. This is the only part of the VIM that produces a potential field inside the shell.

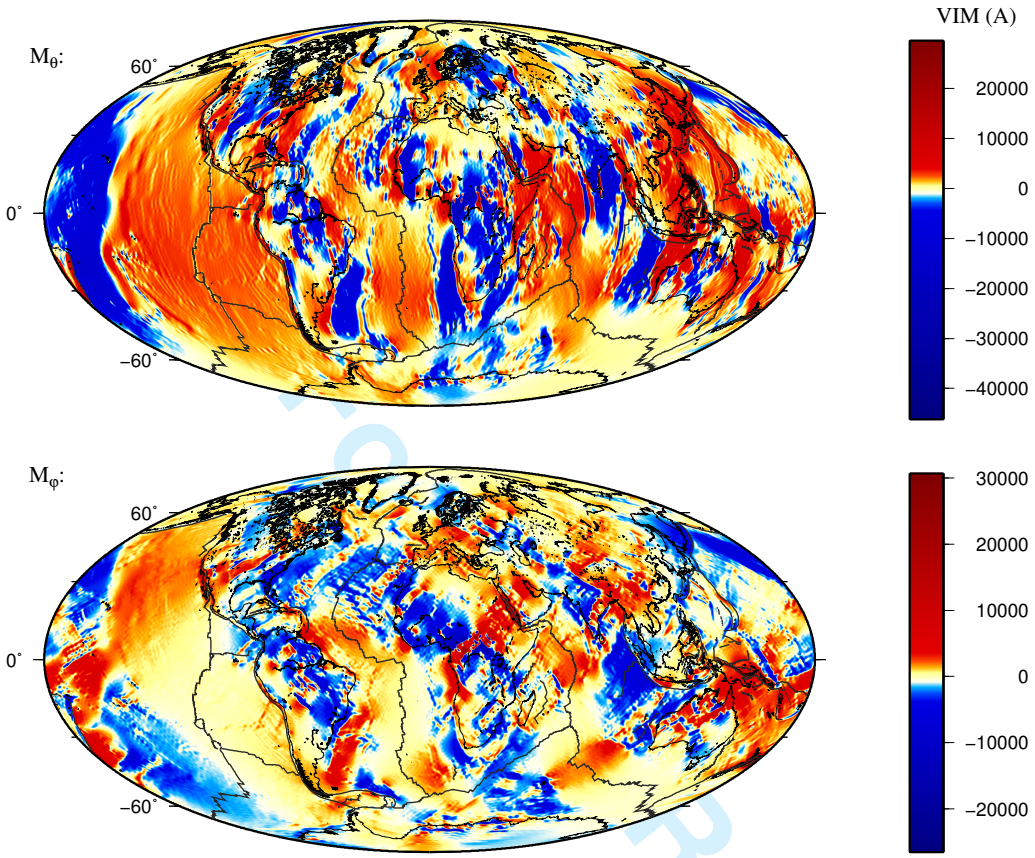

Figure 5. As Figure 3 for the $\mathcal{T}$ component of VIM. This is a toroidal vector that produces no potential magnetic field. The radial component is zero and therefore not shown.

uniqueness because of the two annihilators $\mathcal{E}$ and $\mathcal{T}$. Simple damping will favour $\mathcal{I}$ for no good reason; it is a small part of the total magnetisation. The null space is enormous, comprising any linear combination of $\mathcal{E}$ and $\mathcal{T}$ magnetisations.

Finally, we remark that the dominance of $\mathcal{E}$ may even harm the calculation of magnetic field from a model of crustal magnetisation when calculated by numerical integration using a formula such as (7). The integral over the components $\mathcal{E}$ and $\mathcal{T}$ give zero but will be subject to numerical error, producing leakage into spurious magnetic fields. The leakage may be serious because $\mathcal{E}$ dominates the magnetisation. In this paper we have taken care to do the integration accurately by using a fine (0.25°) grid, finer than is needed for the required resolution, but it is an inefficient way to estimate the field.

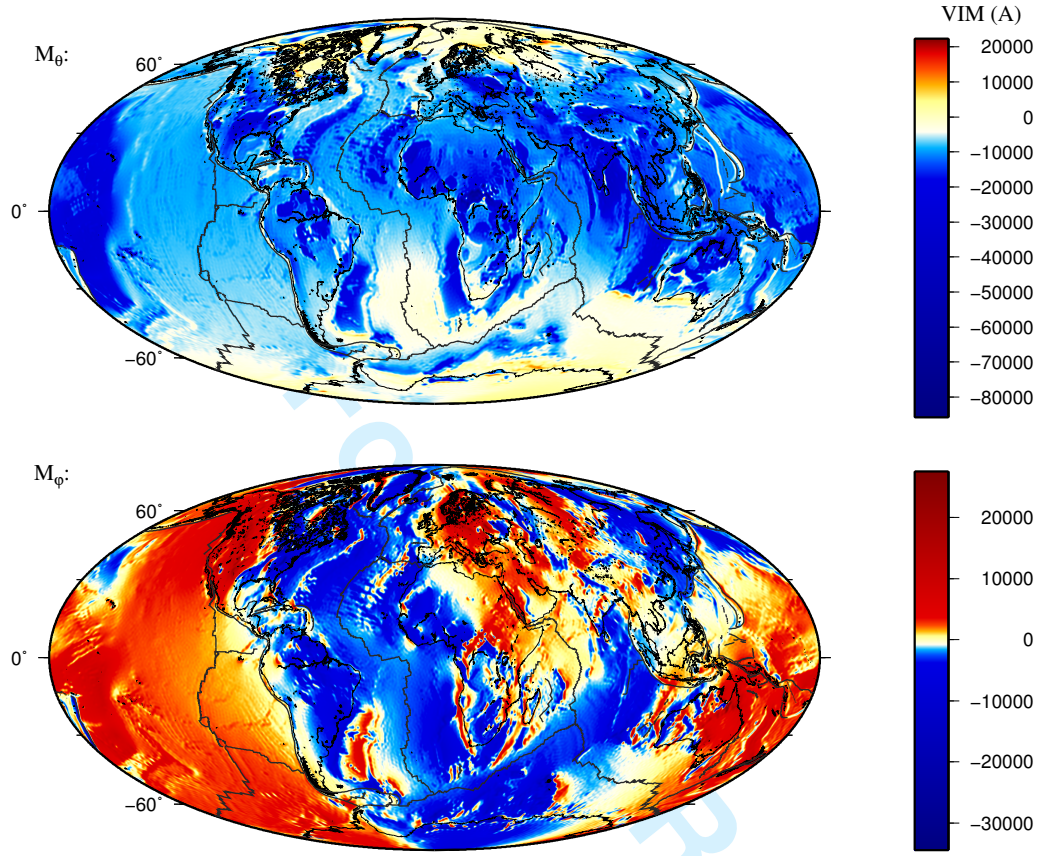

Figure 6. The combined $\mathcal{E}$ and $\mathcal{T}$ components of VIM. This is simply the sum of the magnetisations in Figures 4 and 5; it is that part of the full VIM that produces no potential field outside the shell. The radial component is omitted as it is purely $\mathcal{E}$, the same as the top image of Figure 4.

5.2 Separate behaviour of induced and remanent magnetisations

Our model of VIM has remanence confined to the oceans and an induced component everywhere, which provides an opportunity to study their null spaces separately. The induced and remanent magnetisations were separated and transformed into $\mathcal{I}, \mathcal{E}, \mathcal{T}$ parts. The $\mathcal{E}$ part is even more dominant in the induced magnetisation, with energies in the ratio 89%:8%:3%. There is virtually no signal in the oceans in $\mathcal{I}$ because susceptibility is almost uniform in normal oceanic crust and the underlying mantle (Figure 8). The $\mathcal{E}$ magnetisation is dominated by a large scale reflection of the magnetising IGRF (Figure 9).

It is important to realise that, although the total magnetisation is everywhere parallel to the inducing field, the individual parts $\mathcal{I}, \mathcal{E}, \mathcal{T}$ are not. The minimum norm solution for the magnetisation $\boldsymbol{M}$, given by the $\mathcal{I}$ part, is not the same as the minimum norm solution for $\chi \boldsymbol{B}$, where $\boldsymbol{B}$ is the magnetising field. The inverse problem for a magnetisation that is known

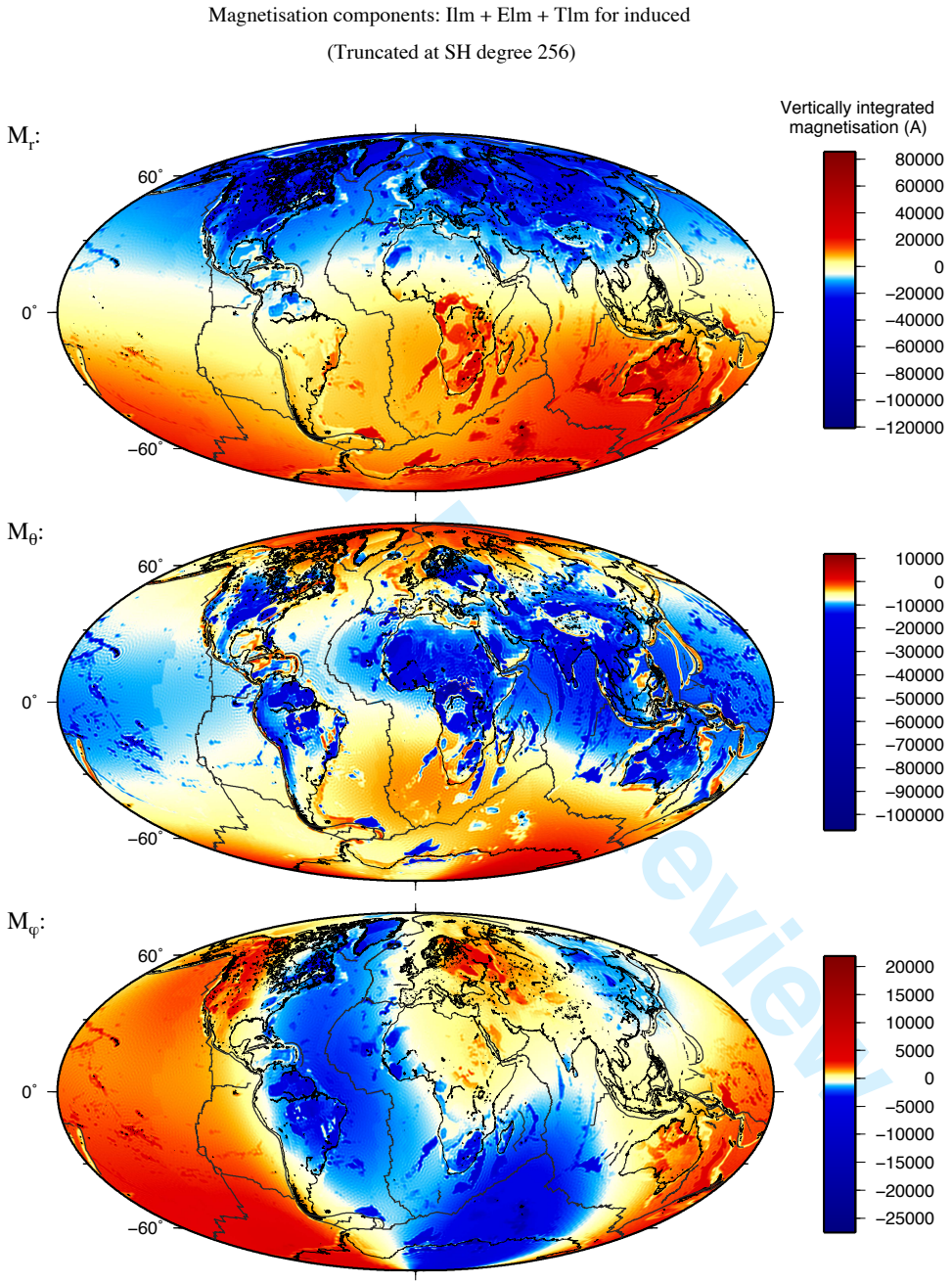

Figure 7. Induced part of the VIM.

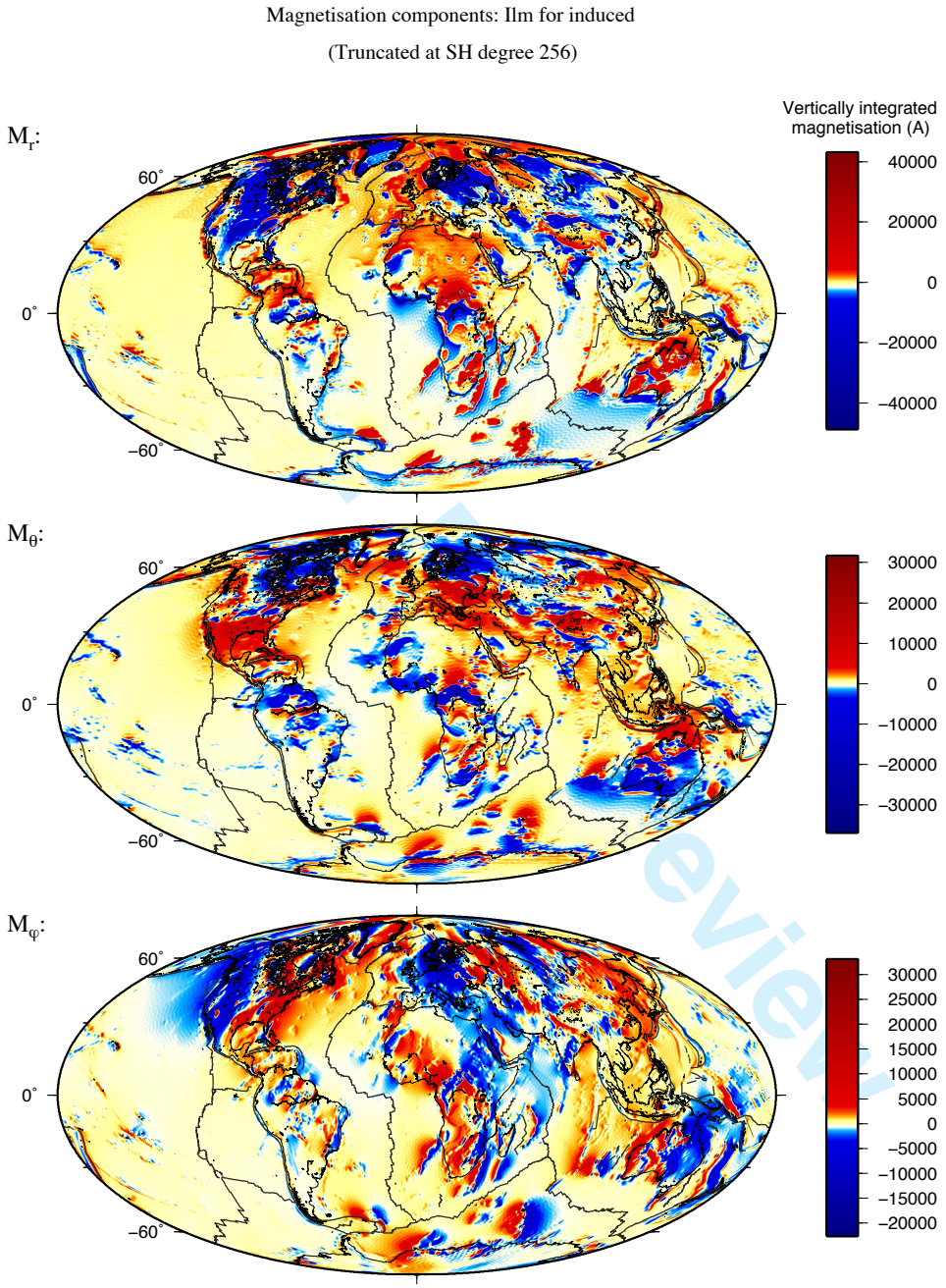

Figure 8. The $\mathcal{I}$ part of the induced VIM

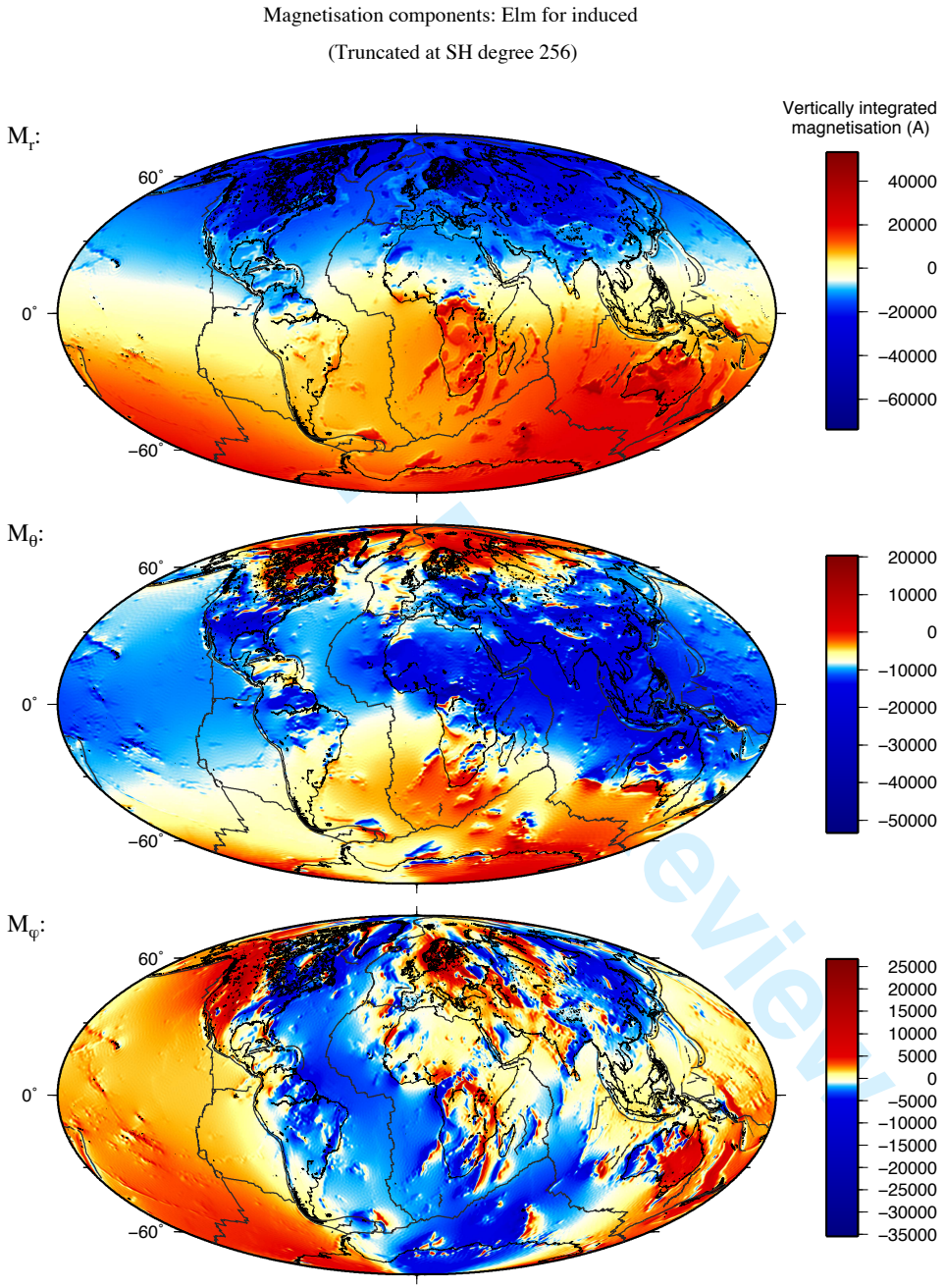

Figure 9. The $\mathcal{E}$ part of the induced VIM.

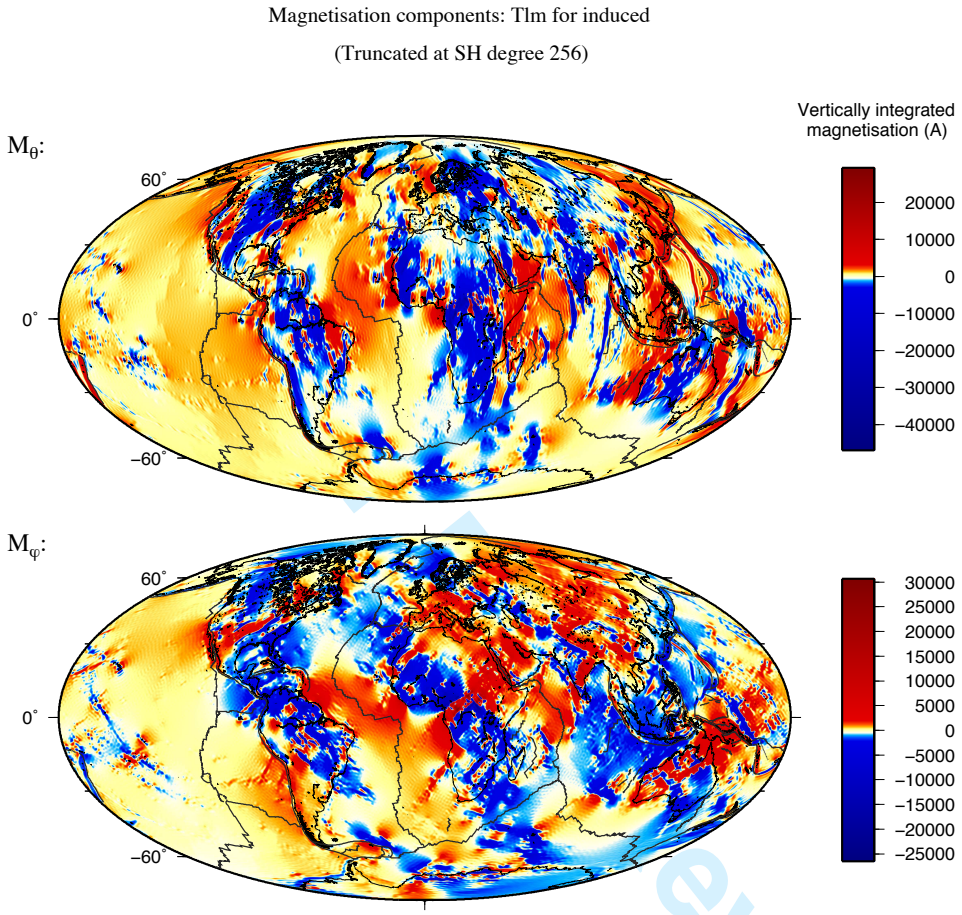

Figure 10. The $\mathcal{T}$ part of the induced VIM.

ahead of time to be purely induced is different from the unconstrained inverse problem and will have a smaller null space because of the additional constraint.

The remanent magnetisation is shown in Figure 11. It is confined to the oceans and dominated by the CQZ regions of the Atlantic margins and western Pacific. In other parts of the oceans the remanence is reduced by the frequent reversals of polarity: adjacent regions of alternating polarity tend to average out at this relatively long length scale. The dipole signature persists but there are substantial azimuthal components resulting from plate rotation, particularly in the western Pacific where the lithosphere is older and has rotated substantially over time.

Remanence is less dominated by the $\mathcal{E}$ part and has a larger toroidal component. The energy ratios are 42%:26%:32%, showing that the plate rotations have had a significant effect on the initial remanence, which would be almost entirely $\mathcal{E}$ because it was constructed from a fairly uniform susceptibility and an internal dipole field. Although the total remanent magnetisation is confined to the oceans (Figure 11), the individual parts $\mathcal{I}, \mathcal{E}, \mathcal{T}$ are not. Note the large signal across southern South America and Africa in the $\mathcal{I}$ part (Figure 12), which is cancelled by similar signals of opposite sign in the $\mathcal{E}$ and $\mathcal{T}$ parts (Figures 13 and 14). The implications for an inversion of magnetic field data would be an apparent degree of remanence over parts of the continents.

6 CONCLUSIONS

The vector spherical harmonics presented here are the natural functions to use for global lithospheric studies because they separate the part of the magnetisation responsible for the observed magnetic field. We have shown that a realistic model of the crustal magnetisation, one derived from first principles using geological information, is dominated by the part that produces a potential magnetic field inside the lithospheric shell and nothing outside it: it produces no observable magnetic field. The vector spherical harmonic formalism isolates the relevant magnetisation, the part that can be refined by improving the fit to available magnetic data, leaving the other part to be determined by other means and with other data. It also provides a simple and fast means of computing the magnetic field from a magnetisation model, and an effective framework to explore the inverse problem of estimating magnetisation from magnetic observations.

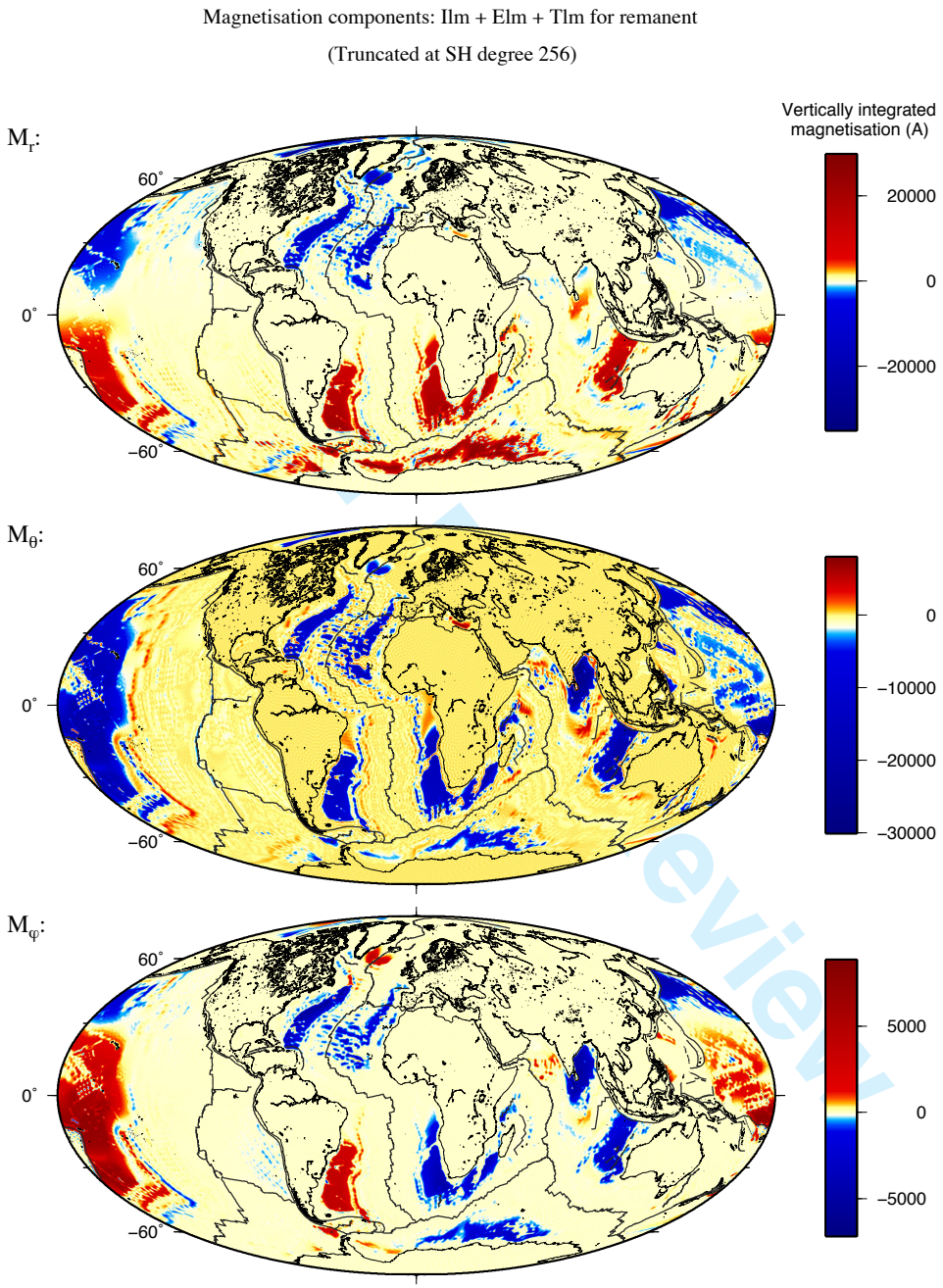

Figure 11. The remanent part of the VIM.

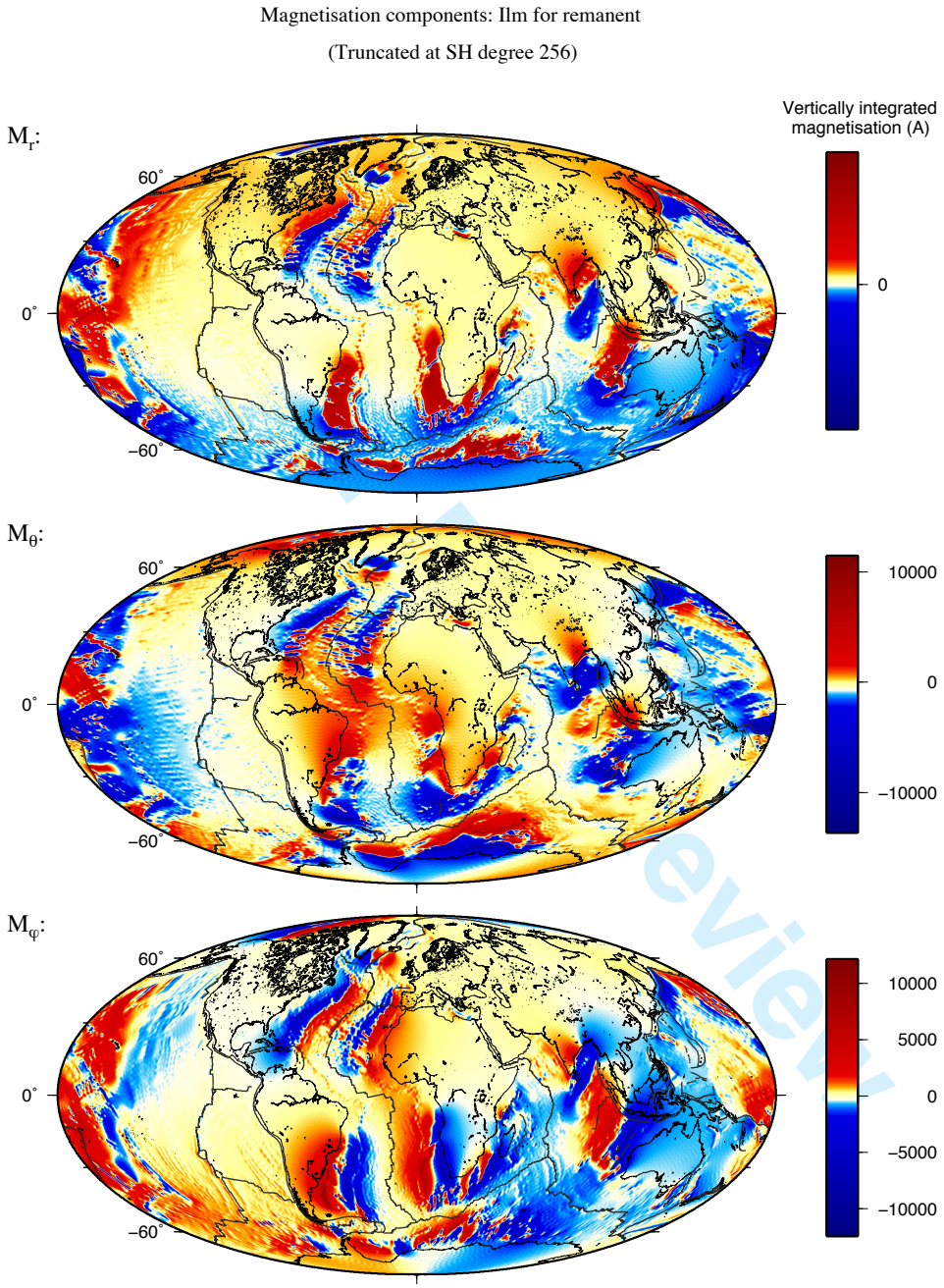

Figure 12. The $\mathcal{I}$ part of the remanent VIM

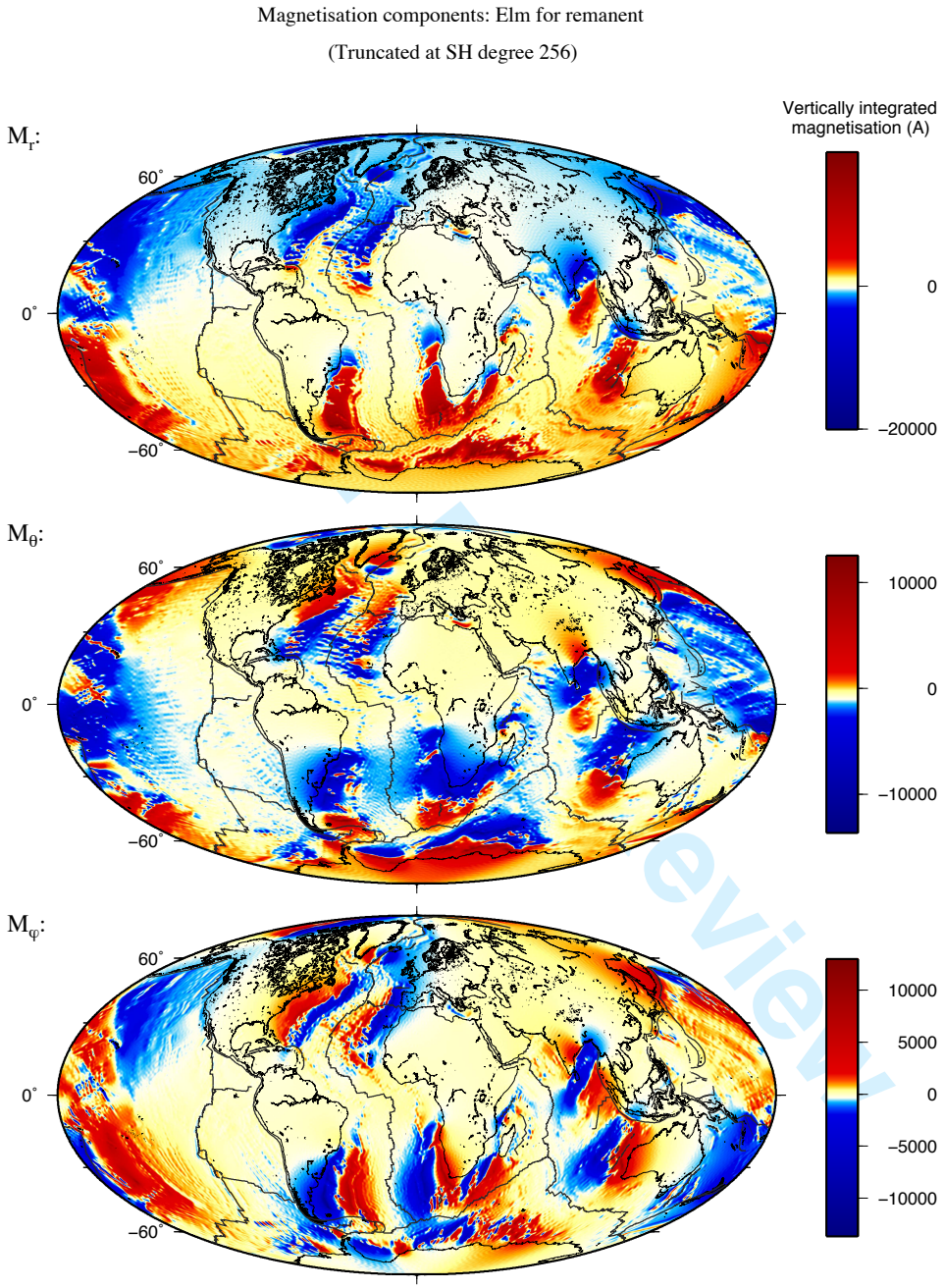

Figure 13. The $\mathcal{E}$ part of the remanent VIM.

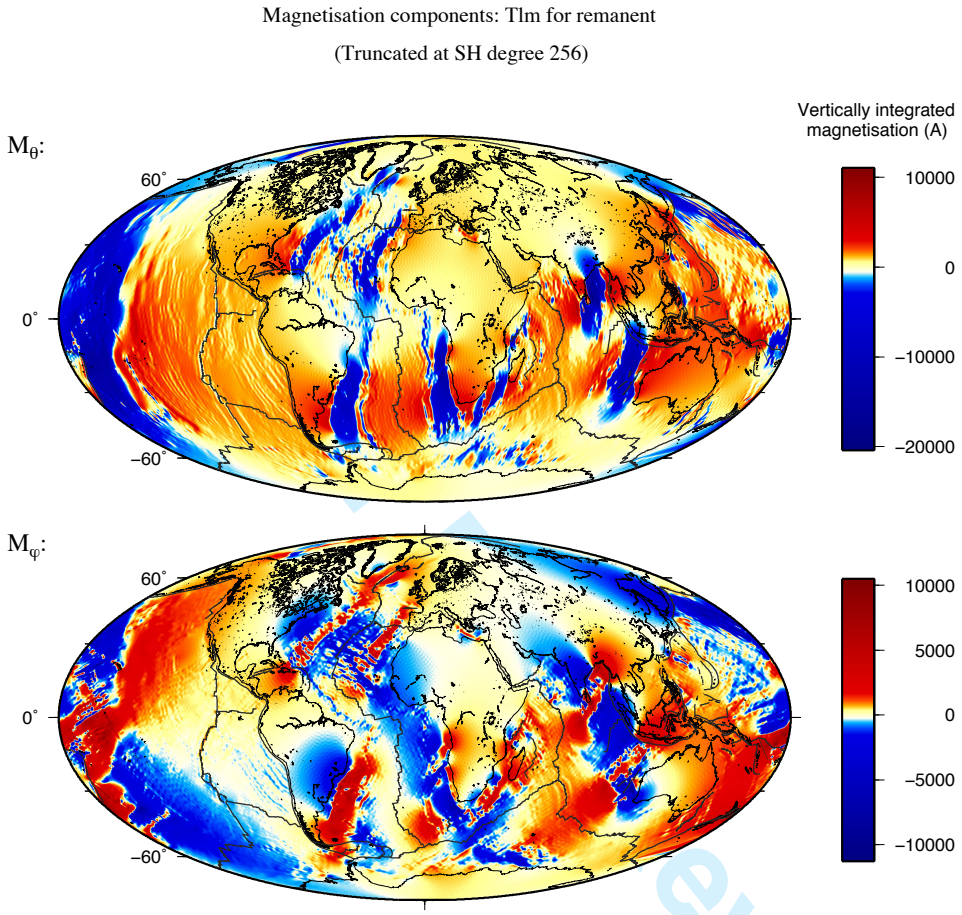

Figure 14. The $\mathcal{T}$ part of the remanent VIM.

ACKNOWLEDGMENTS

We thank Dr. Hemant Kumar for providing us with his model of vertically integrated magnetisation. DG and SM were supported by *GEOSPACE*, NERC consortium grant O/2001/00668. Collaboration with University of Sydney was facilitated by a University of Leeds FIRC grant and a University of Sydney Visiting Fellowship. DG was also supported by the Miller Institute for Basic Research in Science, University of California, Berkeley.

References

Blakely, R. J., 1995, *Potential theory in gravity and magnetic applications*, Cambridge Univ. Press, Cambridge, UK.

Cande, S. C. & Kent, D. V., 1995, Revised calibration of the geomagnetic polarity timescale for the late cretaceous and cenozoic, *J. Geophys. Res.*, **100**, 6093–6095.

Edmonds, A. R., 1974, *Angular Momentum in Quantum Mechanics*, Princeton University Press.

Hemant, K. & Maus, S., 2005, Geological modeling of the new CHAMP magnetic anomaly maps using a geographical information system technique, *J. Geophys. Res.*, **110**, doi:10.1029/2005JB003837.

Jackson, A., 2008, Runcorn's theorem, in *Encyclopaedia of Geomagnetism and Paleomagnetism*, edited by D. Gubbins & E. Herrero-Bervera, pp. 888–889, Springer, Berlin.

Jacobs, J. A., 1994, *Reversals of the Earth's magnetic field*, Cambridge Univ. Press, Cambridge.

Masterson, S., Gubbins, D., Mueller, D., & Hemant, K., 2011, Remanent magnetisation of the oceanic crust, *J. Geophys. Res.*, **In preparation**, xxx.

Masterton, S., 2010, Modelling and interpretation of magnetisation in the oceanic lithosphere, in *PhD Thesis*, University of Leeds.

Meyer, J., Hufen, J.-H., Siebert, M., & Hahn, A., 1983, Investigations of the internal geomagnetic field by means of a global model of the earth's crust, *J. Geophys. - Z. Geophysysik*, **52**, 71–84.

Morse, P. M. & Feschbach, H., 1953, *Methods of Theoretical Physics*, McGraw-Hill.

Raymond, C. A. & Labrecque, J. L., 1987, Magnetisation of the oceanic crust - thermoremanent magnetization of chemical remanent magnetization?, *J. Geophys. Res.*, **92**(B8), 8077–8088.

Runcorn, S., 1975, On the interpretation of lunar magnetism, *Phys. Earth Planet. Int.*.

APPENDIX A: RELATIONS BETWEEN REAL SCHMIDT AND COMPLEX MEAN-NORMALISED SPHERICAL HARMONICS

In geomagnetism the *Schmidt normalisation* of the Associated Legendre functions are commonly used, which have 2 useful orthogonality properties

$$\int_0^\pi P_{l_1}^m P_{l_2}^m \sin\theta \, d\theta = \frac{2\epsilon_m}{2l_1+1}\delta_{l_1 l_2}\delta_{m_1 m_2} \tag{A.1}$$

$$\int_0^\pi \left(\frac{dP_{l_1}^m}{d\theta}\frac{dP_{l_2}^m}{d\theta} + \frac{m^2}{\sin^2\theta} P_{l_1}^m P_{l_2}^m \right) \sin\theta \, d\theta = \frac{2\epsilon_m l\,(l+1)}{(2l+1)}\delta_{l_1 l_2}\delta_{m_1 m_2}, \tag{A.2}$$

where

$$\epsilon_m = 2 - \delta_{m0} \tag{A.3}$$

and δ_{m0} is the usual Kronecker delta. The factor ϵ_m is 1 when $m = 0$ and 2 when $m \neq 0$.

The *real spherical harmonics* are defined by

$$Y_l^{m[c,s]}(\theta,\phi) = P_l^m(\cos\theta)(\cos,\sin)m\phi \tag{A.4}$$

They are orthogonal when integrated over the unit sphere, from the orthogonality of sines and cosines and associated Legendre functions (A.1), and normalise to

$$\oint (Y_l^{m[c,s]})^2 d\Omega = \frac{4\pi}{2l+1} \tag{A.5}$$

The orthogonality condition (A.2) can be used to prove a related orthogonality condition for spherical harmonics

$$\oint \left(\frac{\partial Y_{l_1}^{m_1 c}}{\partial\theta}\frac{\partial Y_{l_2}^{m_2 c}}{\partial\theta} + \frac{1}{\sin^2\theta}\frac{\partial Y_{l_1}^{m_1 c}}{\partial\phi}\frac{\partial Y_{l_2}^{m_2 c}}{\partial\phi} \right) d\Omega = \frac{4\pi l\,(l+1)}{(2l+1)}\delta_{l_1 l_2}\delta_{m_1 m_2} \tag{A.6}$$

and a similar formula for Y_l^{ms}.

The *mean-normalised complex spherical harmonics* are defined by

$$Y_l^m(\theta,\phi) = \sqrt{\frac{2l+1}{\epsilon_m}} P_l^m e^{im\phi}. \tag{A.7}$$

They are related to the real harmonics by

$$Y_l^m = \sqrt{\frac{2l+1}{\epsilon_m}}(Y_l^{mc} + iY_l^{ms}), \tag{A.8}$$

$$Y_l^{mc} = \sqrt{\frac{\epsilon_m}{2l+1}}\mathrm{Re}(Y_l^m), \tag{A.9}$$

$$Y_l^{ms} = \sqrt{\frac{\epsilon_m}{2l+1}}\mathrm{Im}(Y_l^m). \tag{A.10}$$

They normalise to 4π:

$$\oint |Y_l^m|^2 d\Omega = 4\pi. \tag{A.11}$$

APPENDIX B: THE DEFINITE INTEGRAL USED IN SECTION 2

The generating function for Legendre polynomials is

$$\frac{1}{\sqrt{1-2h\cos\Delta+h^2}} = \sum_{l=0}^{\infty} h^l P_l(\cos\Delta), \tag{B.1}$$

where Δ is the angular distance between the points (θ,ϕ) and (θ',ϕ'):

$$\cos\Delta = \cos\theta\cos\theta' + \sin\theta\sin\theta'\cos m(\phi-\phi'). \tag{B.2}$$

The sum rule for Schmidt-normalised associated Legendre functions is

$$P_l(\cos\Delta) = \sum_{m=0}^{l} P_l^m(\cos\theta)P_l^m(\cos\theta')\cos m(\phi-\phi'). \tag{B.3}$$

Expanding out the term $\cos m(\phi-\phi')$ in (B.3) with the usual trigonometric formula and using the notation for spherical harmonics gives

$$P_l(\cos\Delta) = \sum_{m=0}^{l} Y_l^{mc}(\theta,\phi)Y_l^{mc}(\theta',\phi') + Y_l^{ms}(\theta,\phi)Y_l^{ms}(\theta',\phi') \tag{B.4}$$

Substituting into (B.1) gives the generating function for Schmidt-normalised spherical harmonics:

$$\frac{1}{\sqrt{1-2h\cos\Delta+h^2}} = \sum_{l=0}^{\infty} h^l[Y_l^{mc}(\theta,\phi)Y_l^{mc}(\theta',\phi') + Y_l^{ms}(\theta,\phi)Y_l^{ms}(\theta',\phi')] \tag{B.5}$$

Now consider $|\boldsymbol{r}-\boldsymbol{r}'|$, which by the cosine rule is

$$\begin{aligned} |\boldsymbol{r}-\boldsymbol{r}'| &= \sqrt{r^2-2rr'\cos\Delta+r'^2} \\ &= r'\sqrt{1-2(r/r')\cos\Delta+(r/r')^2} \\ &= r\sqrt{1-2(r'/r)\cos\Delta+(r'/r)^2} \end{aligned} \tag{B.6}$$

These expressions yield valid power series in r/r' and r'/r respectively. The second expression in (B.6) gives a convergent power series for $r/r'<1$, the third for $r/r'>1$. For the lithospheric field we require $r>r'$ because the magnetic field is external to the source at $r=r'$. Take the last form, set $h=r'/r$, and combine with (B.5):

$$\frac{1}{|\boldsymbol{r}-\boldsymbol{r}'|} = \frac{1}{r}\sum_{l=0}^{\infty}\left(\frac{r'}{r}\right)^l [Y_l^{mc}(\theta,\phi)Y_l^{mc}(\theta',\phi') + Y_l^{ms}(\theta,\phi)Y_l^{ms}(\theta',\phi')] \tag{B.7}$$

Equation (B.7) may be viewed as the spherical harmonic expansion of $1/|\boldsymbol{r}-\boldsymbol{r}'|$ in $Y_l^{m[c,s]}(\theta,\phi)$ with coefficients

$$\frac{1}{r}\left(\frac{r'}{r}\right)^l Y_l^{m[c,s]}(\theta',\phi')$$

Multiplying both sides of (B.7) by $Y_l^{m[c,s]}(\theta,\phi)$, integrating over Ω, and using orthogonality of the spherical harmonics therefore gives

$$\oint \frac{Y_l^{m[c,s]}(\theta,\phi)}{|\boldsymbol{r}-\boldsymbol{r}'|} d\Omega = \frac{4\pi}{2l+1}\frac{1}{r}\left(\frac{r'}{r}\right)^l Y_l^{m[c,s]}(\theta',\phi') \tag{B.8}$$

which is the integral in (6).

Another form is obtained from the sum valid for $r < r'$

$$\oint \frac{Y_l^{m[c,s]}(\theta,\phi)}{|\boldsymbol{r}-\boldsymbol{r}'|} d\Omega = \frac{4\pi}{2l+1}\frac{1}{r'}\left(\frac{r}{r'}\right)^l Y_l^{m[c,s]}(\theta',\phi') \tag{B.9}$$

which is the integral in (14).